Phase Field Simulation for Recrystallization Kinetics of Cold-Drawn 0.12wt%C Steel in Full Annealing

Nurudeen A. Raji, Oluleke O. Oluwole

Abstract-The importance of recrystallization kinetics in metal process cannot be over emphasized in providing information as to the control of microstructure of materials for purpose of improving or impacting desired mechanical properties in processed materials. In this study, 0.12wt% C steel cold drawn between 20% - 55% were graduallyheateduptoatemperatureof900°C followed bysoakingtreatment between 600 seconds and 3600 seconds in a Gallenkomp® mufflefurnace model SVL-1009 with voltage regulation of 220 V, 50 Hz of temperature range 300°C - 1000°C. The influence of the annealing process on the strength and impact toughness properties of the annealed steel were evaluated from tensile and charpy-impact testsconductedontheannealedsteel.A phase field method is used to describe the recrystallization kinetics of the annealed cold drawn 0.12wt%C steel for the different degrees of cold drawn deformation.The experimental data obtained from the tensile and charpy-impact test were used as input data for the phase field simulation of the recrystallization process. The results show that the yield strength of the annealed cold drawn 0.12wt% C steel increases with increasing soaking time within the range of 600 sec.– 3600 sec. for the 20% cold drawn steel, between 600 sec.- 2400 sec. for the 25% and between 600 sec.-1800 sec. for the 40% and 55% cold drawn steel. The treatment increased the impact toughness of the steel for the 20%-40% cold drawn deformation but loses its toughness for the 55% cold drawn steel. The tensile strength however reduces for all the cold drawn steel irrespective of the degree of deformation.The simulation results show that reformation of grains in cold drawn 0.12wt%C steel depends on the degree of cold drawn deformation and the soaking time of annealing. The response of the mechanical properties of the annealed cold drawn 0.12wt% C steel therefore depends on the degree of cold deformation and soaking time of annealing.

Keywords: Cold-drawn, annealed, soaking time, yield strength, tensile strength, impact toughness, recrystallization.

1 INTRODUCTION

Drawn steel are products of metal drawing process which include bar or rod drawing, tube drawing and wire drawing. This drawing process has been widely used to manufacture fine wires, tension loaded structural components, springs, paper clips, spokes for wheels and plain nails [1],[2].

The wire drawing process is used to reduce the cross-section of a wire by pulling the wire through series of drawing dies of decreasing diameter to produce wires of desired diameter as is obtainable in the manufacture of plain nails of 4 inches, 3 inches, 2½ inches and 2 inches,. It is mostly performed at room temperature and thus is classified as cold-work process.

The original metal usually consists of strain-free crystal grains [3]. When the metal is deformed by drawing, dislocation and other imperfections such as vacancies are introduced into the crystal structure generating microstructure heterogeneities that exhibit large orientation gradient [4]. The accumulation of dislocation at the grain boundary results in stored energy within the structure. The grains also acquire a preferred orientation or texture. The structural changes which occur include the gradual stretching of the grains in the direction of principal deformation. The performance of the drawn steel in service and during manufacture is determined by their microstructure and crystallographic orientation[5]. The microstructure which occurs depends on the degree of deformation [6].

The wire hardens during the wire drawing process and the ductility of the wire reduces while the tensile strength increases [7]. The hardness is usually due to the generation of the dislocation and the movement of the dislocations within the material structure as the deformation progresses. This defect is known as strain hardening. The strain hardening also known as work hardening is an increment in internal energy associated with an increase in the dislocation density as well as

- *Nurudeen A. Raji is currently pursuing PhD degree program in Mechanical engineering in University of Ibadan, Nigeria. E-mail: kunle_raji@yahoo.com*
- *Dr. Oluleke O. Oluwole is a Senior Lecturer in the Mechanical engineering department of the University of Ibadan, Nigeria. E-mail: oluwoleo2@asme.org*

density in point defects, such as vacancies and interstitials [8],[9]. These changes in the mechanical properties of the steel due to the deformation often influence the performance of the resulting product of the process in service. The focus of the research is on plain nails manufactured from low carbon steel in Nigeria.

The manufacture of nails include drawing low carbon steel wire through a series of drawing dies to reduce the diameter of the wire or rod to the desired diameter of the nails. During the drawing operation the carbon steel experiences microstructure changes which affect the mechanical properties of the steel and consequently the performance of the nail product in service. The associated problems include high strain hardening of the steel due to the degree of plastic deformation which causes nail brittleness or poor ductility resulting in buckling of the nail in service. The large amount of internal strain in the form dislocation as a result of the strain hardening means that energy is stored in the metal. This energy can be released through heat treatment, where energy in the form of heat is introduced into the material allowing the release of stored energy in the process of recrystallization [10].

Recrystallization is a thermally activated process, consisting of the generation of strain-free grains and their growth at the expense of the deformed grains until the deform grain is entirely consumed[11]. And the driving force for recrystallization is the energy stored in the material during deformation[12]

The purpose of recrystallization is to refine the grains for improved properties. Computational model could be developed for purpose of optimizing the recrystallization process for improved mechanical properties of the material and the phase field method is such model that could be used to achieve these. The model could be used to predict microstructure evolution in terms of grain size during recrystallization process.

Recrystallization modeling using the phase field method with particular application to 0.012%wt% C steel is considered in this research.The generally accepted empirical model which is used to describe recrystallization kinetics is the Johnson-Mehl-Avrami-Kolmogorov (JMAK)[6]. The model was developed on the assumption that the recrystallized nuclei form randomly in the cold-worked microstructure and that the growth of the nuclei is isotropic but real material do not exhibit this behavior because of the non-uniform distribution of the stored energy, non-random distribution of the nuclei and anisotropic growth of recrystallized nuclei [13]. It is therefore of importance to consider real situation of the recrystallization process through experimentation as input for a realistic model. The phase field model has become a powerful tool in describing complex microstructure evolution.

In the phase field model, the entire microstructure is described by the combination of its deformed grains, recrystallized grains, grain boundaries, and the diffused interface region which describes the transition of the deformed grains to recrystallized grains.

The stored energy in the system could be represented by its total Gibb's energy 'F' of the system and is usually expressed as a functional of all field variables of the system [14], [15].

Phase-field model is a method which could be used to describe microstructure evolution in processed materials. The phase field describes the evolution of microstructure with time. The entire microstructure of the system is described by three distinct quantities; the precipitate, the matrix, and the interface. In the case of recrystallization process of polycrystalline materials the three quantities could be considered as the recrystallized grain, the deformed grains, and the interface which is a region over which a deformed grain changes to recrystallized grain. The entire microstructure is represented by a continuous variable ϕ, known as order parameter which varies between $\phi = 0$ for the deformed grain and $\phi = 1$ for the recrystallized grain while the interface is a range of value $0 < \phi < 1$. The interfacial region is a mixture of the deformed matrix and the recrystallizing grain. The set of values of the ordered parameter over the whole microstructure is the phase field.

Phase field model have been extensively used to model a number of physical phenomena such as in solidification process [16], [17], [18], [19], [20], hydrodynamic of incompressible fluid mixture [21], [22], Phase transformation [23], multi-phase systems [24], [25], [26] among the numerous studies carried out on this new line of material engineering design..

The energy stored in the microstructure during cold deformation serves as the driving force for recrystallization which requires lowering this energy to achieve stability. The energy could be described as the functional of the phase field parameter ϕas expressed in equation (1) described by Cahn-Hilliard theory also known as the Ginzburg-Landau free energy theory. The expression wasderived by using the first and second order limits of a Taylor series expansion model as discussed in [27], [28], [29].

$$F = \int \left[f(\phi) + \frac{\alpha^2}{2} |\nabla \phi|^2 \right] dV \qquad (1)$$

F is known as Gibbs free energy for heterogeneous system, $f(\phi)$is the free energy density which describes the energy of the bulk matrix. The gradient term,$\frac{\alpha^2}{2}|\nabla\phi|^2$, expresses the penalty for interfaces, and

necessarily results in both a surface energy and finite non-zero interface width [30]. αis known as the gradient energy coefficient which serve as the penalty to ensures that the energy within the structure decreases as recrystallization progresses.

The energy functional expression of equation (1) is usually obtained by Taylor series expansion as detailed in [29].The free energy is used to derive recrystallization kinetic which require that the total energy decreases monotonically in time such that $\frac{\delta F}{\delta t} \leq 0$.

The major difference between different phase field models is in the construction of the local free energy as a function of the phase field. This is determined experimentally in this research specifically for the 0.12wt%C steel used for the manufacture of plain nails.

The function f(ϕ) has the shape of a double-well [31] at ϕ which defines the minima as ϕ=0 for the deformed matrix and $\phi = 1$ for the recrystallized grain. The function f(ϕ) is postulated as a function of the phase field parameters as expressed [32], [33]and is expressed as;

$$f(\phi) = \big(1 - p(\phi)\big)f_m(\rho_a) + p(\phi)f_r(\rho_a) + wq(\phi) \quad (2)$$

Where q(ϕ) and p(ϕ) known as double-well function and interpolation function respectively are standard set of functions which are usually chosen as expressed in equations (3) and (4) to ensure that $\frac{\partial f(\phi)}{\partial \phi} = 0$ when $\phi = 0$ and $\phi = 1$ for all temperature [34]

$$q(\phi) = \phi^2(1-\phi)^2 \quad (3)$$

with minima at $\phi = 0$ and 1, scaled by the well height w which is the kinetic barrier between the two minima,

$$p(\phi) = \phi^3(10 - 15\phi + 6\phi^2) \quad (4)$$

These expressions of equations (3) and (4) have been widely used in phase-field models [35, 36]. The procedure for the selection of the functions could be obtained in [37]. The function p(ϕ) describes the release of the energy in the system as recrystallization proceed and is defined so that the minima of the non-conserved ordered parameter are satisfied such that;

$p(0) = 0$, $p(1) = 1$ and $p'(0) = p'(1) = 0$

$f_m(\rho_a)$is the stored energy in the deformed matrix

$f_r(\rho_a)$is the stored energy in the recrystallized grain

$f_r(\rho_a)$ could be taking to be zero knowing that a recrystallized grain is free of defect, thus

$f_m(\rho_a) = E_{stored}$.Hence,

$$f(\phi) = \big(1 - p(\phi)\big)E_{stored} + wq(\phi) \quad (5)$$

The evolution of the microstructure could therefore be described by the field parameters; ϕ which describes the evolution of the grain structure during the recrystallization process. The microstructure evolution equations for the field parameter is time dependent expressions which guarantee a decrease in the total free energy to ensure the equilibrium of the system and is usually determined by the Allen-Cahn evolution theory otherwise known as Ginsburg-Landau evolution theory which states that the flux is proportional to the driving force and expressed as in [38].

$$\frac{1}{M_\phi}\frac{\partial \phi}{\partial t} = -\frac{\delta F}{\delta \phi} \quad (6)$$

Where, $\frac{1}{M_\phi}$ is a positive constant termed as the mobility of the phase parameter.

The model adopted here is due to [39,40]. However for many materials, including metals, the surface energy of the interface and the mobility depend on orientation. These effects were assumed negligible and not accounted for in this expression assuming a uniaxial loading in service of the 0.12wt%c steel under consideration.

$$\frac{\partial \phi}{\partial t} = M_\phi\left[\alpha^2\nabla^2\phi - \frac{\partial f(\phi)}{\partial \phi}\right] \quad (7)$$

Where $M_\phi$is the phase field mobility.

Equation (7) is the model required for the simulation of the phase field and could be solved using the finite difference method under specified material parameters which are obtained from the full annealing experimentation. The phase field parameters are related to the material parameters as follows [29, 31, 34];

$$\alpha = \sqrt{\frac{3\delta\sigma}{b}}, \qquad w = \frac{6\sigma b}{\delta}$$

σ= Yield energy, δ= interface thickness, b=constant determined from the mobility of the interface region.

2 MATERIALS AND METHODS

2.1 Experimental Procedure

In this study, commercially available wire rod specimens drawn from as-received wire of 5.5 mm diameter to nominal diameter of 3.24 mm were selected as materials for the study. The chemical composition of the cold- drawn low carbon steel is presented in Table 1. A Muffle furnace, Gallenkomp® model SVL-1009 with voltage regulation of 220 V, 50 Hz of temperature range 300°C - 1000°C obtained in the materials test laboratory of Igbinedion University, Okada was used for the annealing process. The tensile tests were done at room temperature on an Instron® 3369 testing machine equipped with an electro-mechanical sensor for control of tensile strain in the active zone of samples in the load range up to 50 kN.

Specimens of the cold-drawn carbon steel at 20%, 25%, 40% and 55% degree of deformation were investigated. The specimens were cut to a length of 45 mm for purpose of the tensile tests and were annealed at temperature of 900°C for time intervals ranging from 600sec. to 3600sec. All the specimens were cooled in the furnace down to the ambient temperature of 27°C and were then removed for testing.

The relative toughness at the different annealing soaking time was determined from the Charpy impact tests. For reproducibility of results, the test was done using three samples for each soaking time. The mean of the measurements were taken of the data with minima measured standard error.

Table1:Chemicalcompositionoftheas-receivedsteelwirematerial used (% wt).

Element	C	Si	Mn	P	Fe
%	0.12	0.18	0.14	0.7	98.86

The Samplescutfrom theannealedwire were taken throughagrindingprocess using siliconcarbide paper,240,320,400,and 600gritand polishedinitiallyat1µmandfinallyat0.5µmusingemery clothandsilicon-carbidesolution andetchedwith2%nital.Opticalmicroscope (OM) withimage capturingdevicewasusedtoobservethemicrostructureof boththecold drawnand theannealed specimens.Theplanimetricprocedure forthegraincountingmethodwasusedtomeasurethe meangrain-sizefrom theobtainedmicrographsasdescribedin[41].The sampleswerealsosubjectedtotensiletestsonauniversal testingmachineInstron3369witha loadcapacityof50kNtoobtainthestrength-ductility propertiesofthesamplesatthedifferent soakingtime.Thesampleswere alsotestedforimpacttoughnessandhardness withincreasing degreeofcold deformationasdescribed in[42].

2.2 Phase Field Model

The free energy functional for the deformed matrix of the low carbon steel is considered to be the sum of two energy parts as expressed;

$$F = F_1(\phi) + F_{int}(\phi) \quad (8)$$

$F_1(\phi)$is the energy due to the bulk material. This energy combines the energy of the deformed matrix and the energy of the recrystallizing grain. $F_{int}(\phi)$ is the interfacial energy.The functional is usually defined as integrals of the form [43];

$$F_i = \int f_i(\phi, \nabla\phi, \ldots\ldots)dV \quad (9)$$

The system is said to be in equilibrium at $\frac{\partial\varphi}{\partial t} = 0$ which is obtained at constant values of the order parameter $\varphi = 0$ for deformed matrix and $\varphi = 1$ for recrystallized grains[34].For a single –phase solid such as been considered here, the equilibrium equation of equation (7) is obtained as;

$$\alpha^2 \frac{d^2\phi}{dx^2} - \frac{\partial g(\phi)}{\partial \phi} = 0 \quad (10)$$

An exact solution could be obtained for one dimensional transition zone as[29];

$$\phi(x) = \frac{1}{2}\left[1 + \tanh\left(\frac{i\Delta x}{2(2w)^{1/2}\alpha}\right)\right] \quad (11)$$

The finite difference method could also be used to build a recurrence relation of the phase field function for a two dimensional system. The method provides an approximation to the value of the unknown function at a number of discrete points in the domain of the phase field problem.

Equation (7) is solved using the finite difference method as follows;
For time discretization;

$$\frac{\partial\phi}{\partial t} = \frac{\phi^{n+1}(i,j) - \phi^n(i,j)}{\Delta t}$$

For space discretization;

$$\nabla^2\phi(i,j) = \frac{1}{\Delta x^2}[\phi(i+1,j) + \phi(i-1,j) + \phi(i,j+1) + \phi(i,j-1) - 4\varphi(i,j)]$$

3 EXPERIMENTAL RESULTS AND COMPUTATIONAL MODEL

3.1 Phase Field Simulation for Recrystallization kinetics

The recrystallization kinetics is represented by the phase field equation (7) for the grain evolution in annealing. The material parameters are obtained from the experimental data given in Tables2-7

TABLE 2
MECHANICAL PROPERTIES OF AS-RECEIVED 0.12WT%C STEEL.

	% deformation	Grain boundary energy (J)	Yield strength (MPa)	Tensile strength (MPa)	Impact Toughness (J)
Control specimen	20	34.596	300	805	15.5
	25	26.776	250	745	7.07
	40	7.482	200	690	3.97
	55	7.272	160	665	3.57

TABLE 3
MECHANICAL PROPERTIES OF COLD DRAWN0.12WT% C STEEL ANNEALED AT 900DEG. C FOR 600 SEC.

	% deformation	Grain boundary energy (J)	Yield strength (MPa)	Tensile strength (MPa)	Impact Toughness (J)
Annealing time of 600 sec.	20	68.853	405.2828	490.11	17.5
	25	44.164	0.76	380.08	8.5
	40	0.747	200.89	290.01	5.2
	55	0.1719	85.21	185.55	2.3

TABLE 4
MECHANICAL PROPERTIES OF COLD DRAWN 0.12WT%C STEEL ANNEALED AT 900DEG. C FOR 1200 SEC.

	% deformation	Grain boundary energy (J)	Yield strength (MPa)	Tensile strength (MPa)	Impact Toughness (J)
Annealing time of 1200 sec.	20	53.965	415.0825	510.09	14.5
	25	41.875	0.99	375.66	5.0
	40	25.311	200.74	280.81	3.7
	55	11.283	130.99	180.50	2.8

TABLE 5

MECHANICAL PROPERTIES OF COLD DRAWN0.12WT% C ANNEALED AT 900DEG. C FOR 1800 SEC.

Annealing time of 1800 sec.	% deformation	Grain boundary energy (J)	Yield strength (MPa)	Tensile strength (MPa)	Impact Toughness (J)
	20	46.411	450.96	650.42	19.2
	25	26.756	248.76	355.44	6.9
	40	23.642	195.02	275.96	5.0
	55	13.034	140.91	180.01	4.8

TABLE6
MECHANICAL PROPERTIES OF COLD DRAWN 0.12WT%C STEEL ANNEALED AT 900DEG. C FOR 2400 SEC

Annealing time of 2400 sec.	% deformation	Grain boundary energy (J)	Yield strength (MPa)	Tensile strength (MPa)	Impact Toughness (J)
	20	74.713	445.99	700.09	12.3
	25	14.15	208.67	260.00	5.5
	40	20.343	190.56	260.98	3.2
	55	14.284	150.05	225.11	2.8

TABLE 7
MECHANICAL PROPERTIES OF COLD DRAWN 0.12WT% C ANNEALED AT 900DEG. C FOR 3000 SEC.

Annealing time of 3000 sec.	% deformation	Grain boundary energy (J)	Yield strength (MPa)	Tensile strength (MPa)	Impact Toughness (J)
	20	55.627	380.03	525.00	13.5
	25	39.105	270.11	325.16	5.0
	40	22.226	187.92	280.09	4.2
	55	7.5573	150.55	180.61	3.8

TABLE 8
MECHANICAL PROPERTIES OF COLD DRAWN 0.12WT%C STEEL ANNEALED AT 900DEG. C FOR 3600 SEC

Annealing time of 2400 sec.	% deformation	Grain boundary energy (J)	Yield strength (MPa)	Tensile strength (MPa)	Impact Toughness (J)
	20	76.415	350.16	680.13	14
	25	36.419	150.51	375.99	7
	40	22.587	180.04	270.99	3
	55	10.542	120.98	180.46	2.6

Interface thickness of δ = 8.1 nm is selected for purpose of this model. There is no strict rule as to the selection of the interface thickness which is usually adjusted to minimize computational expenses [29].The variables required for the phase field parameters are obtained from the experimental data as detailed in Table 9.These parameters serve as input to the model equation(11).

TABLE 9
PHASE FIELD PARAMETERS OBTAINED FROM EXPERIMENTAL DATA OF THE MATERIAL PROPERTIES

Phase Field Parameter for annealed 0.12wt%C at 900 deg. C	% Degree of cold drawn deformation			
	20	25	40	55
Energy gradient (J/s)	4.904	4.192	2.31	1.95
Potential height (μm)	3.421	2.501	7.59	5.42
Yield Energy (J)	67.7	49	15.01	10.7

Fig. 1,2,3, 4 shows the recrystallization kinetics for grain size evolution for the 20%, 25%, 40% and 55% Cold- drawn deformation respectively.

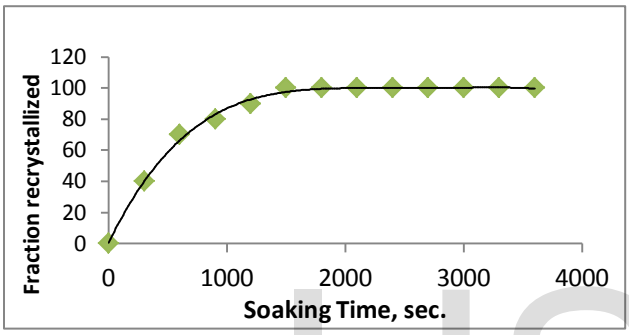

Fig.1. Phase Field simulation curve for recrystallized volume fraction of 20% cold drawn 0.12wt%C steel annealed at 900 deg. C.

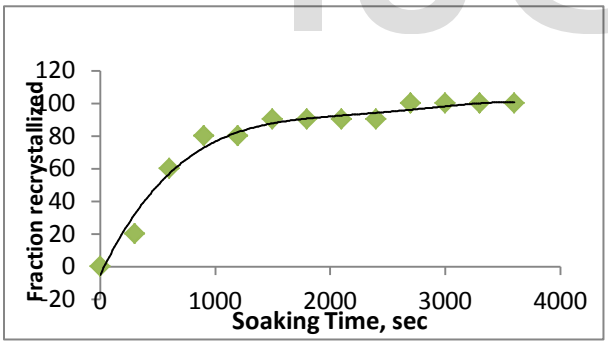

Fig. 2: Phase Field simulation curve for recrystallized volume fraction of 25% cold drawn 0.12wt% C steel annealed at 900 deg. C.

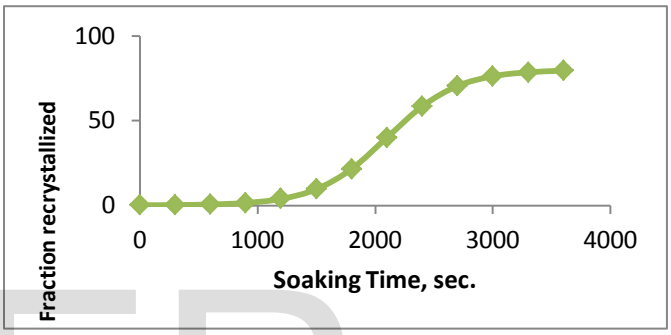

Fig. 3. Phase Field simulation curve for recrystallized volume fraction of 40% cold drawn 0.12wt% C steel annealed at 900 deg. C.

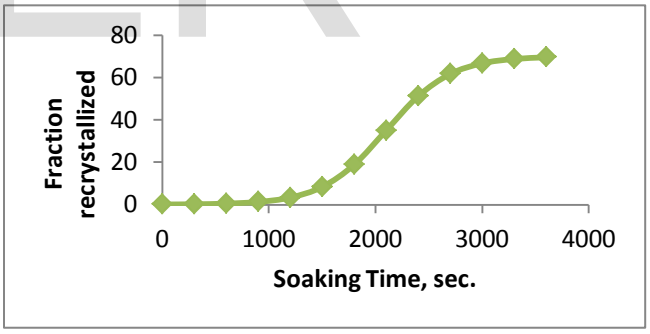

Fig. 4: Phase Field simulation curve for recrystallized volume fraction of 55% cold drawn 0.12wt% C steel annealed at 900 deg. C.

Comparison of the recrystallization curves shows that the % degree of cold drawn deformation of the steel contributes to the kinetics of the grain reformation. The rate at which the grains recrystallize reduces with the degree of cold drawn deformation for 0.12wt% C steel. This implies that at lower degree of cold drawn deformation, the accumulated dislocation defects are quickly annihilated during the recovery process. The recrystallization kinetics of the annealed steel for the 20% and 25% degree of deformation did not indicate a clear nucleation period as compared with the 40% and 55% degree of deformation. This implies that nucleation sites are pronounced in the 40% and 50% degree of drawn deformation. This explains the time taking for sub-grains formation in the 40% and 55% valued at 1300 seconds and 1500 seconds respectively. This is justified by increasing strain hardening parameter with increasing degree of cold drawn deformation as discussed in [44]. Thisphenomenon invariable affects the mechanical properties of the

annealed cold drawn 0.12wt% C steel as observed in Fig. 5–16.

3.2 Influence of full annealing on mechanical properties of cold drawn 0.12wt% C steel

Fig. 5-16 show how the mechanical properties respond to the annealing of cold drawn 0.12wt%C steel at 900 deg. C for varying soaking time ranging from 600 seconds to 3600 seconds.

Annealing of cold drawn 0.12wt%C steel influences the strength and impact toughness of the steel considerably. Annealing at 900 deg. C within the range of 600 seconds and 3600 seconds involves increase in the yield strength of the 20% cold drawn steel for the whole temperature range of 600 seconds – 3600 seconds as shown in Figure 5a.

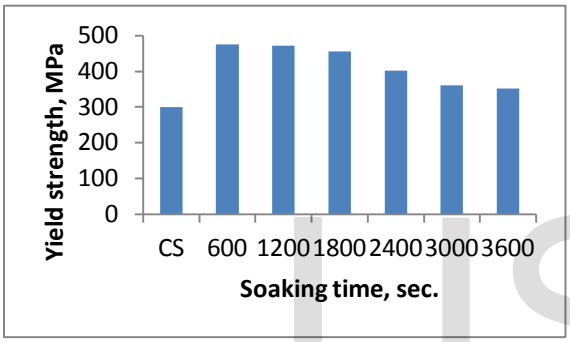

(a)

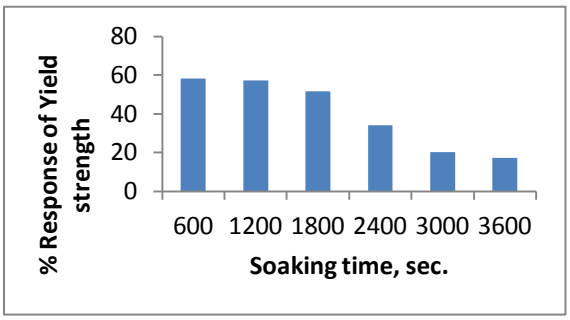

(b)

Fig. 5.Influence of Yield strength on annealed 20% cold drawn 0.12wt% C
(a) Yield strength of annealed 20% cold drawn 0.12wt% C steel compared to the control sample (CS)
(b) Percentage response of yield strength of 20% cold drawn 0.12wt% C steel annealed at 900 deg. C

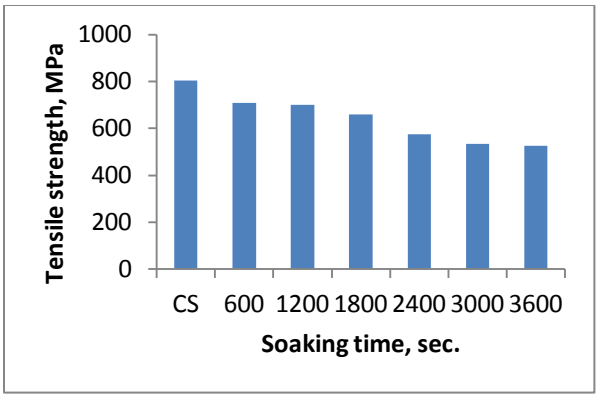

(a)

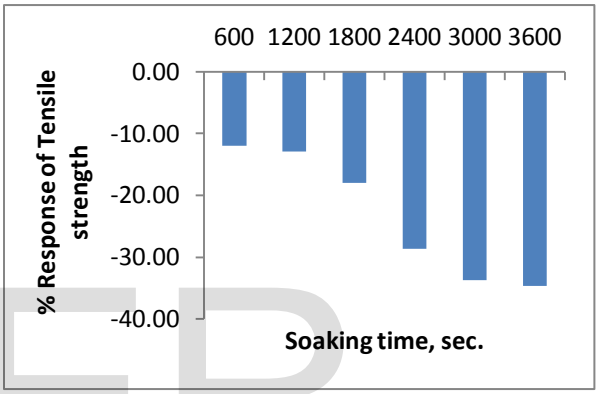

(b)

Fig. 6. Influence of Tensile strength on annealed 20% cold drawn 0.12wt% C
(a) Tensile strength of annealed 20% cold drawn 0.12wt% C steel compared to the control sample (CS)
(b) Percentage response of tensile strength of 20% cold drawn 0.12wt% C steel annealed at 900 deg. C

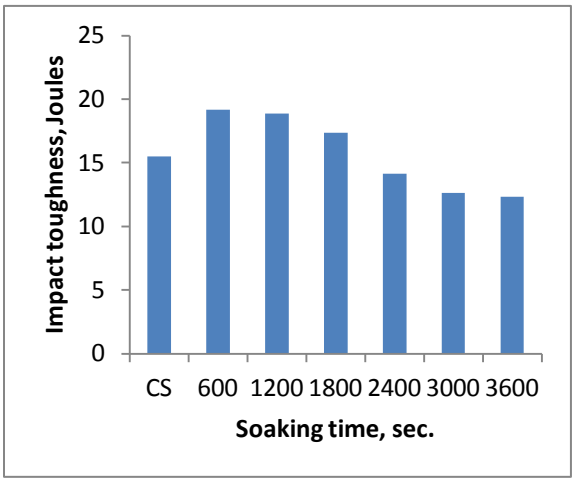

(a)

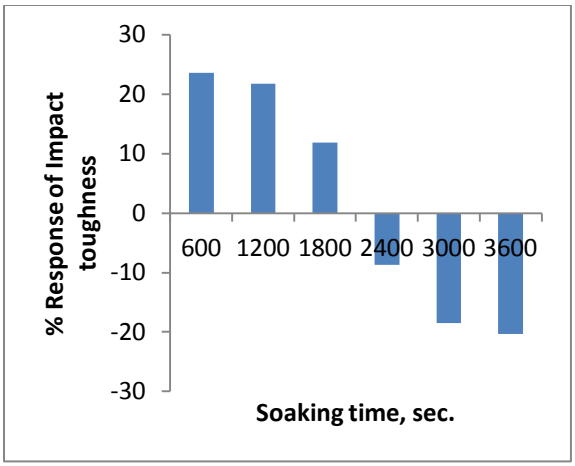

(b)

Fig. 7. Influence of Impact toughness on annealed 20% cold drawn 0.12wt% C
(a) Impact toughness of annealed 20% cold drawn 0.12wt% C steel compared to the control sample (CS)
(b) Percentage response of Impact toughness of 20% cold drawn 0.12wt% C steel annealed at 900deg. C

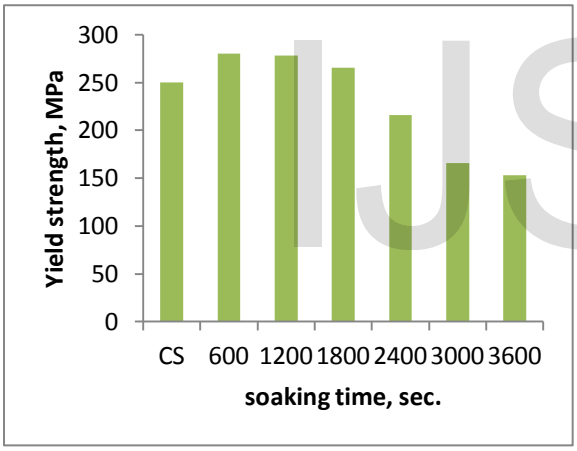

(a)

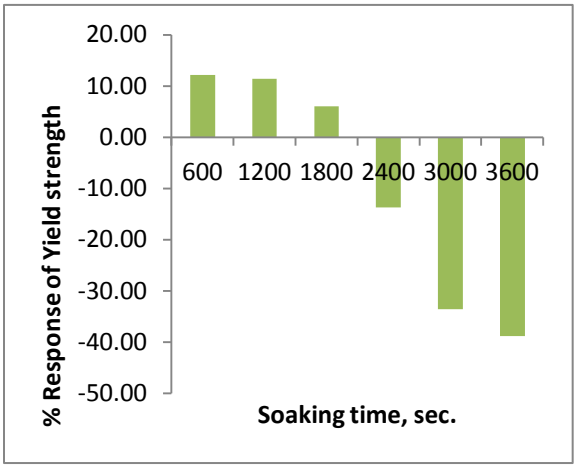

(b)

Fig.8. Influence of Yield strength on annealed 25% cold drawn 0.12wt% C
(a) Yield strength of annealed 25% cold drawn 0.12wt% C steel compared to the control sample (CS)
(b) Percentage response of yield strength of 25% cold drawn 0.12wt% C steel annealed at 900 deg. C

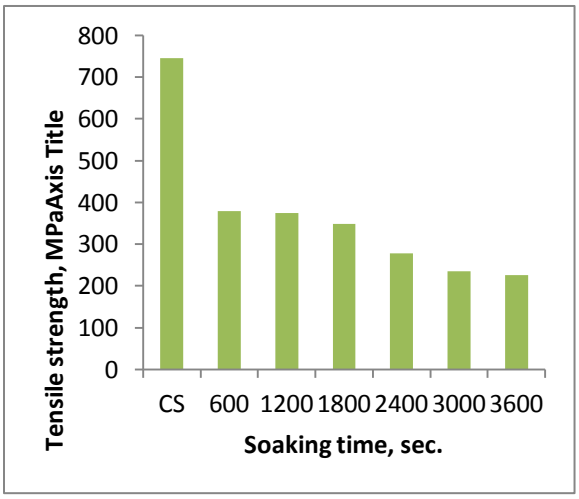

(a)

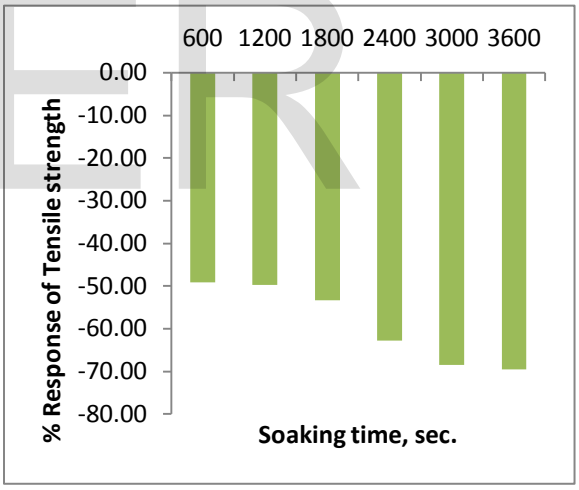

(b)

Fig. 9. Influence of Tensile strength on annealed 25% cold drawn 0.12wt% C
(a) Tensile strength of annealed 25% cold drawn 0.12wt% C steel compared to the control sample (CS)
(b) Percentage response of tensile strength of 25% cold drawn 0.12wt% C steel annealed at 900 deg. C

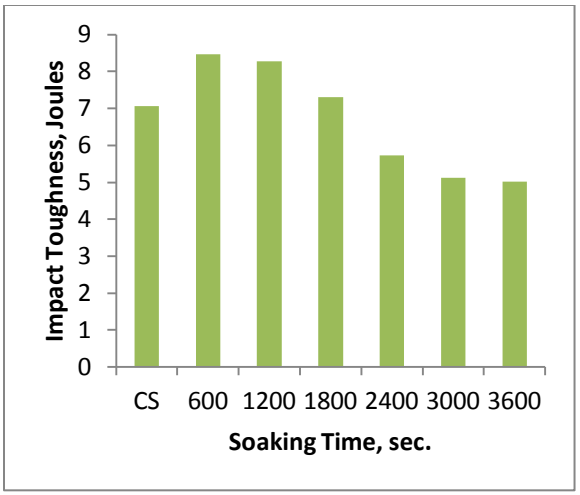

(a)

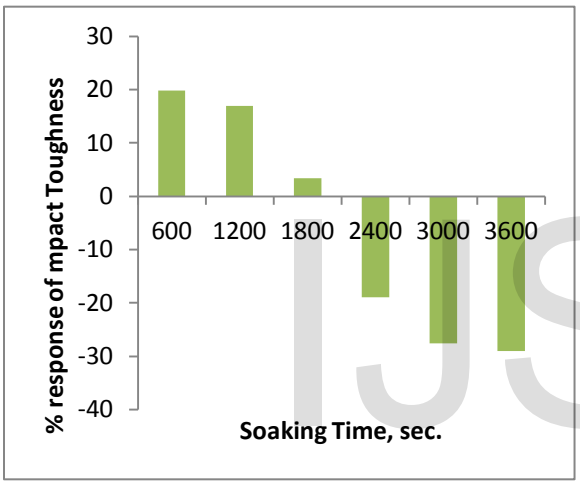

(b)

Fig. 10.Influence of Impact toughness on annealed 25% cold drawn 0.12wt% C
(a) Impact toughness of annealed 25% cold drawn 0.12wt% C steel compared to the control sample (CS)
(b) Percentage response of Impact toughness of 25% cold drawn 0.12wt% C steel annealed at 900deg. C

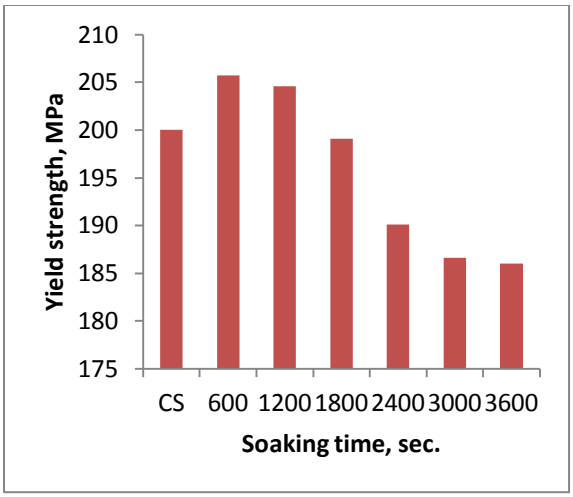

(a)

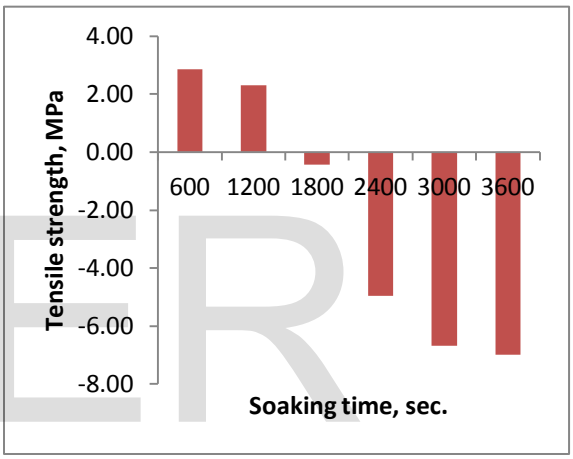

(b)

Fig. 11.Influence of Yield strength on annealed 40% cold drawn 0.12wt% C
(a) Yield strength of annealed 40% cold drawn 0.12wt% C steel compared to the control sample (CS)
(b) Percentage response of yield strength of 40% cold drawn 0.12wt% C steel annealed at 900 deg. C

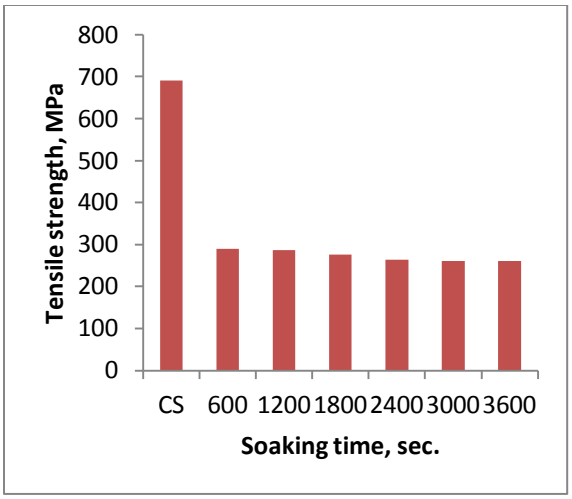

(a)

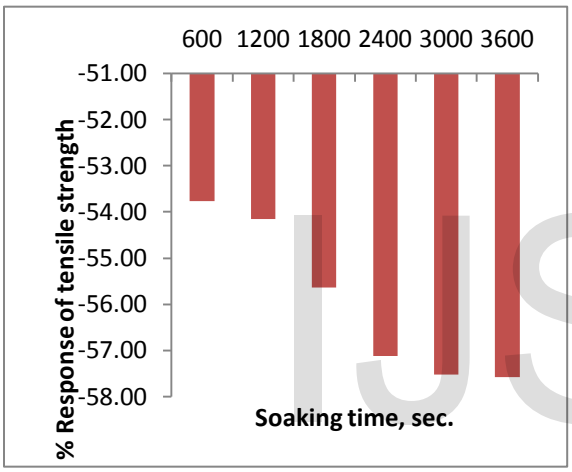

(b)

Fig. 12. Influence of Tensile strength on annealed 40% cold drawn 0.12wt% C
(a) Tensile strength of annealed 40% cold drawn 0.12wt% C steel compared to the control sample (CS)
(b) Percentage response of Tensile strength of 40% cold drawn 0.12wt% C steel annealed at 900 deg. C

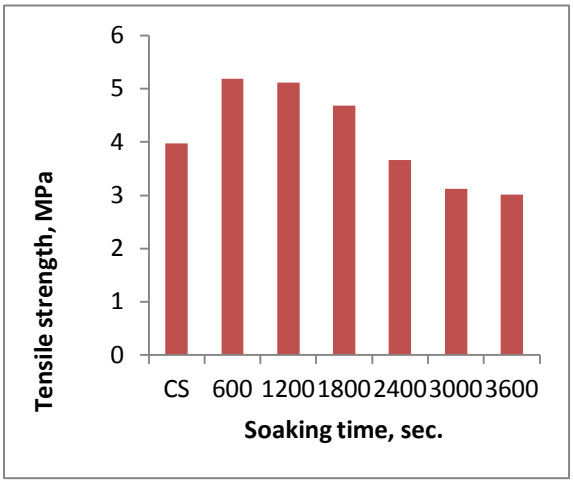

(a)

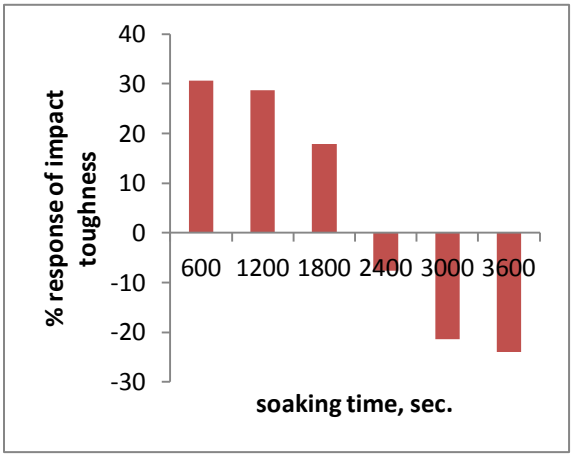

(b)

Fig. 13. Influence of Impact toughness on annealed 40% cold drawn 0.12wt% C
(a) Impact toughness of annealed 40% cold drawn 0.12wt% C steel compared to the control sample (CS)
(b) Percentage response of Impact toughness of 40% cold drawn 0.12wt% C steel annealed at 900deg. C

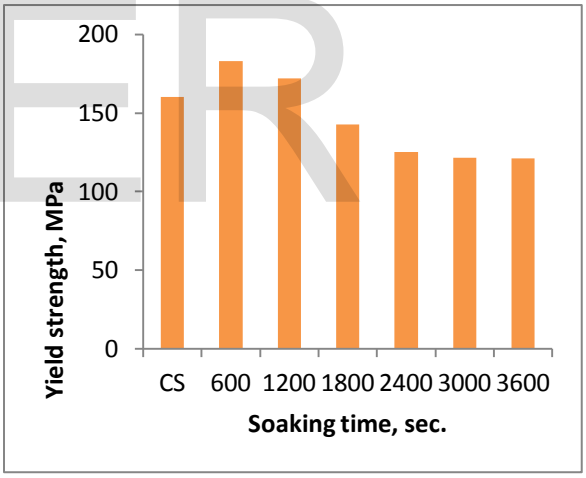

(a)

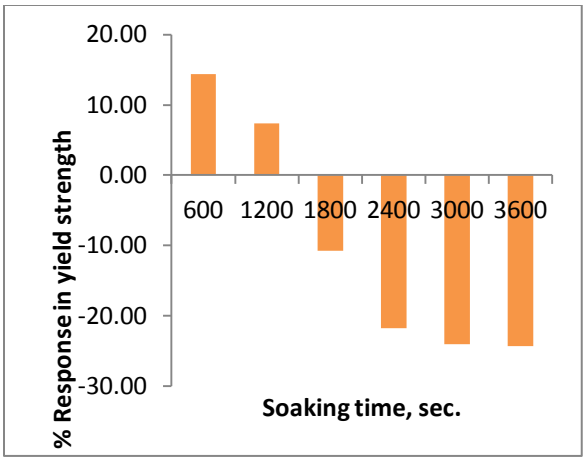

(b)

Fig. 14. Influence of Yield strength on annealed 55% cold drawn 0.12wt% C
(a) Yield strength of annealed 55% cold drawn 0.12wt% C steel compared to the control sample (CS)
(b) Percentage response of yield strength of 55% cold drawn 0.12wt% C steel annealed at 900 deg. C

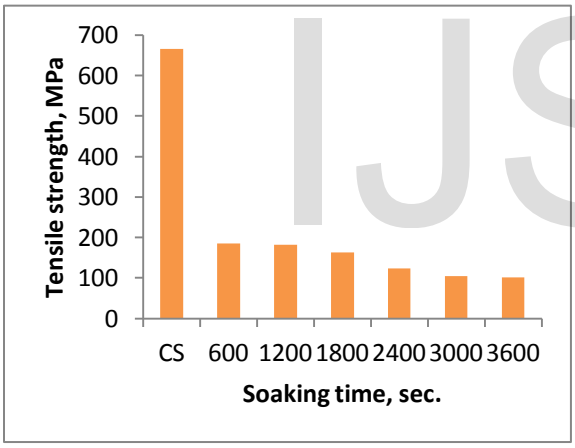

(a)

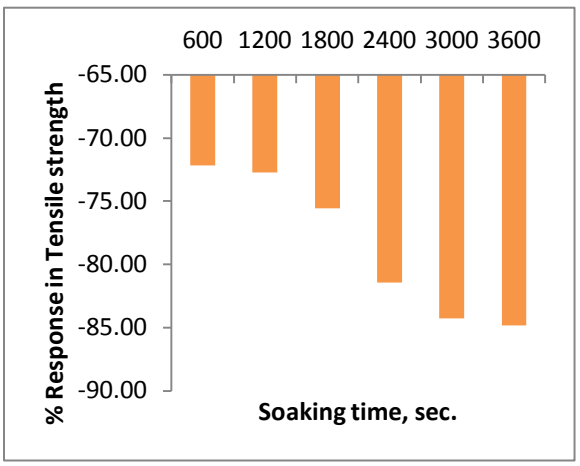

(b)

Figure 15: Influence of Tensile strength on annealed 55% cold drawn 0.12wt% C
(a) Tensile strength of annealed 55% cold drawn 0.12wt% C steel compared to the control sample (CS)
(b) Percentage response of Tensile strength of 55% cold drawn 0.12wt% C steel annealed at 900 deg. C

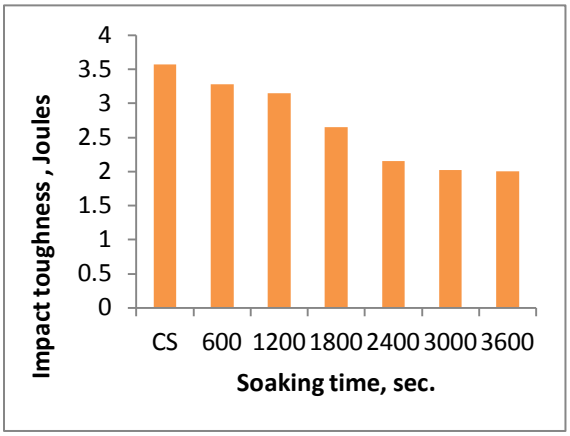

(a)

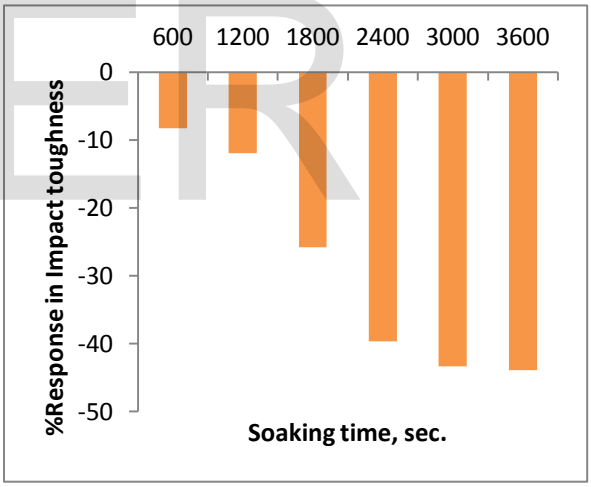

(b)

Figure 16: Influence of Impact toughness on annealed 55% cold drawn 0.12wt% C
(a) Impact toughness of annealed 55% cold drawn 0.12wt% C steel compared to the control sample (CS)
(b) Percentage response of Impact toughness of 55% cold drawn 0.12wt% C steel annealed at 900deg. C

However the rate at which the yield strength increases for the 20% degree of cold-drawing reduces with increasing soaking time as shown in Fig. 5b. annealing of the 25%, 40%, and 55% cold drawn steel only causes increase in yield strength of the steels within certain range of soaking time after which the

steels reduces in yield strength as shown in Figures 8a, 11a and 14a. specifically the yield strength of the annealed 25% cold-drawn steel increases within 600 seconds to 1800 seconds after which the yield strength begins to reduce within soaking time range of 2400 seconds to 3600 seconds as shown in Fig. 8b. Similar observation is made with the annealed 40% and 55% cold- drawn steel as shown in Fig. 11 and 14 where reduction in yield strength occur within the soaking time range of 1800 seconds to 3600 seconds. The rate of reduction of the yield strength also increases with increasing degree of deformation.

Similar observation is made with the impact toughness of the annealed cold drawn steel for the 20%, 25% and 40% cold drawn deformation where the toughness of the annealed steel reduces considerable within soaking time range of 2400 seconds to 3600 seconds as shown in Fig. 7b, 10b, and 13b but increases in impact toughness within soaking time range of 600 seconds and 1800 seconds as shown in Fig. 7a, 10a and 13a respectively. However the annealed 55% degree cold drawn steel lost its impact toughness considerably within the whole soaking time range of 600 seconds to 3600 seconds as shown in Figure 16.

The tensile strength of the annealed cold drawn 0.12wt% C steel at 900 deg. C drops considerably with increasing soaking time. The rate at which the tensile strength reduces however also depends on the degree of cold deformation of the steel as shown in Figures 6, 9, 12, and 15.

It could be inferred from the results that grain growth takes place in the annealed 0.12wt% C steel causing the drop in the yield strength and impact toughness of the steels when annealed at 900 deg. C. However grain growth in the annealed cold drawn steel commence at different range of soaking time depending on the degree of cold drawn deformation. It could also be inferred that improved tensile properties and impact toughness of the annealed steel could be achieved by controlling the recrystallized fraction of the steels for different degree of cold drawn deformation. This could be achieved by optimizing the percentage recrystallized fraction of the annealed steel.

4 CONCLUSION

The investigation of the influence of annealing at 900 deg. Celcius at soaking time range within 600 sec.-3600sec. on cold drawn deformed 0.12wt% C steel shows that the annealing within the soaking time range of 600 sec. – 3600 sec. involves considerable reduction in the tensile strength of the cold drawn 0.12wt% C steel. The rate at which tensile strength reduces also increases with increasing soaking time but a considerable increase in the yield strength within soaking time range of 600 sec.–3600 sec. for the 20% deformation, 600 sec.–1800 sec. for the 25% deformation but 600 sec.–1200 sec. for the 40% and 55% cold drawn steel.Also the annealing process impact considerable increase on the impact toughness of the cold drawn steel. The impact toughness of the steel increases considerable between soaking time of 600 sec.–1800 sec. for the cold deformation of 20% - 40% although at different rate and between soaking time range of 600 sec. – 1200 sec. for the 55% deformed steel. This implies that yield strength and impact toughness of annealed cold drawn 0.12wt%C steel depends not only on the degree of cold drawn deformation but also on the soaking time of annealing. The recrystallization kinetics of the grain growth for the different degrees of cold drawn deformation shows that nucleation process is more pronounced in the 40% and 55% degree of cold deformation indicating accumulation of more dislocation defect at the grain boundaries.

REFERENCES

[1] E. N. Popova, V. V. Popov, E. P. Romanov, N. E. Hle-bova and A. K. Shikov, "Effect of Deformation and An-nealing on Texture Parametal of Composite Cu-Nb Wire," ScuptaMaterialia, Vol. 51, pp. 727-731, 2004. doi:10.1016/j.scriptamat.2004.05.037

[2] F. Yan, C. Ma, J. Q. Jiang, H. P. Feng and S. T. Zha, "Effect of Cumulative Strain on Texture Characteristics during Wire Drawing of Eutectoid Steels," Scripta Mate-rialia, Vol. 59 pp. 850-853, 2008,. doi:10.1016/j.scriptamat.2008.06.048

[3] F. J. Humphreys and M. Hatherly, "Recrystallization and Related Annealing Phenomena," 2nd Edition Elsevier Ltd. U. K., 2004.

[4] M. Ferry, "Influence of Fine Particle of Grain Coarsening within an Orientation Gradient," ActaMaterialia, Vol. 53, pp. 773-783, 2005. doi:10.1016/j.actamat.2004.10.030

[5] N. Peranio, F. Roters and D. Raabe, Microstructure evolution during recrystallization in dual-phase steels, Materials Science Forum, Vols. 715-716, pp 13-22, 2012. doi:10.4028/www.scientific.net/MSF.715-716.13

[6] P.N. Kalu and D.R. Waryoba, "A JMAK-microhardness model for quantifying the kinetics of restoration mechanisms in inhomogeneous microstructure," Materials Science and Engineering A 464, pp. 68–75, 2007. doi:10.1016/j.msea.2007.01.124

[7] A. Phelippeau, S. Pommier, T. Tsakalakos and M.P.C. Clavel, "Cold drawn steel wires—processing, residual stresses and ductility—part I: metallography and finite element analyses," Fatigue Fracture Engineering Material Structure, vol. 29, pp. 243–253, 2006. DOI:10.1111/j.1460-2695.2005.00981.x

[8] A. L. R. de Castro, H. B. Campos and P. R. Cetlin, "In-fluence of Die Semi-Angle on Mechanical Properties of Single and Multiple Pass Drawn Copper," Journal of Materials Process

and Technology, Vol. 60, pp. 179-182, 1996. Doi:10.1016/0924-0136(96)02325-4.

[9] D. G. Cram, H. S. Zurob, Y. J. M. Brechet and C. R. Hutchinsm, "Modeling Discontinuous Dynamic Recrys-tallization Using a Physically Based Model for Nuclea-tion," Acta. Materialia, Vol. 57, pp. 5218-5228, 2009. doi:10.1016/j.actamat.2009.07.024

[10] M. Janošec, I. Schindler, V. Vodárek, J. Palát, S.Rusz, P.Suchánek, M. Růžička, E. Místecký and N. Huť, "Microstructure and mechanical properties of cold rolled,annealed HSLA strip steels,"Archives of civil and mechanical engineering. vol. 7(2), pp. 29-38, 2007.

[11] H. Hallberg, "Approaches to Modeling of Recrystallization," Metals, vol. 1, pp. 16-48, 2011. doi:10.3390/met1010016

[12] Y. L ü , D.A.Molodov and G. Gottstein, "Recrystallization kinetics and microstructure evolution duringannealing of a cold-rolled Fe–Mn–C alloy,"ActaMaterialia, vol. 59, pp. 3229–3243, 2011.doi:10.1016/j.actamat.2011.01.063

[13] B. Radhakrishnan, G.B. Sarma and T. Zacharia, "Modeling the kinetics and microstructure evolution during static recrystallization-Monte Carlo simulation of recrystallization," ActaMaterialia, vol. 46(12), pp. 4415-4433, 1998.http://dx.doi.org/10.1016/S1359-6454(98)00077-9,

[14] M.K. Venkitachalam, L.-Q.Chen, A.G. Khachaturyan and G.L. Messing, "A multiple-component order parameter phase field model for anisotropic grain growth," Materials Science and Engineering A238, pp.94-100, 1997.http://dx.doi.org/10.1016/S0921-5093(97)00443-7

[15] N. Moelans, B. Blanpan and P. Wollants, "An introduction to phase-field modeling of microstructure evolution.Computer coupling phase diagrams and thermochemistry," vol. 32, pp. 268-294, 2008. doi:10.1016/j.calphad.2007.11.003.

[16] D.M. Anderson, G.B. McFadden and A.A. Wheeler, "A phase-field model of solidification with convection," Physica D, vol. 135, pp. 175–194, 2000.http://dx.doi.org/10.1016/S0167-2789(99)00109-8

[17] I. Loginova, J. Agren, and G. Amberg, "On the formation of Widmanstätten ferrite in binary Fe–C phase-field approach" Acta Materialia, vol. 52, pp. 4055–4063, 2004. doi:10.1016/j.actamat.2004.05.033

[18] Y. B. Altundasand G. Caginalp, "Computations of Dendrites in 3-D and Comparison with Microgravity Experiments," Journal of Statistical Physics, Vol. 110, Nos. 3–6, pp. 1055-1067, 2003.DOI: 10.1023/A:1022140725763

[19] R. Zhang, T. Jing,W.Jie, and B. Liu, "Phase-field simulation of solidification in multicomponent alloys coupled with thermodynamic and diffusion mobility databases ActaMaterialia, vol. 54, pp. 2235–2239,2006. doi:10.1016/j.actamat.2006.01.029

[20] Y. Zhang, W. Zhang, T. Wang, L. Fan and C. Wang,"Phase field modeling of dendritic coarsening during isothermal solidification,"ChinaFoundry, vol. 8, no. 3, pp. 313-315,2011. www.intechopen.com

[21] P. Yue, J.J. Feng, C. Liu and J. Shen, "A diffuse-interface method for simulating two-phase flows of complex fluids," Journal of Fluid Mechanics, vol. 515, pp. 293–317, 2004.doi: 10.1017/S0022112004000370

[22] Z. Zhang and H. Tang, "An adaptive phase field method for the mixture of two incompressible fluids," Computers and Fluids, vol. 36, pp.1307–1318, 2007. doi:10.1016/j.compfluid.2006.12.003

[23] K. Ammar, B. Appolaire, G. Cailletaud, and S. Forest, "Phase field modeling of elasto-plastic deformation induced by diffusion controlled growth of a misfitting spherical precipitate," Philosophical Magazine Letters, vol. 91, no. 3, pp. 164 — 172, 2011. doi.org/10.1080/09500839.2010.541891

[24] H.-J. Diepers, C. Beckermann, and I. Steinbach, "Simulation of convection and ripening in a binary alloy mush using the phase-field method," Actamaterialia, Vol. 47, No. 13, pp. 3663-3678, 1999.doi.org/10.1016/S1359-6454(99)00239-6

[25] S.G. Kim, "A phase-field model with anti-trapping current for multicomponent alloys with arbitrary thermodynamic properties," ActaMaterialia, vol. 55, pp. 4391–4399, 2007.doi:10.1016/j.actamat.2007.04.004

[26] H. Kobayashi, M. Ode, S.G. Kim, W.T. Kim and T. Suzuki, "Phase-field model for solidification of ternary alloys coupled with thermodynamic database," ScriptaMaterialia, vol. 48, pp. 689–694, 2003.www.sciencedirect.com/science/article/pii/S1359646202005572

[27] D. Kessler, "Sharp interface limits of a thermodynamically consistent solutal phase field model. " Journal of Crystal Growth, vol. 224, pp. 175–186, 2001.www.sciencedirect.com/science/article/pii/S0022024801008144

[28] J. Rosam, P.K. Jimack and A. Mullis, "A fully implicit, fully adaptive time and space discretization method for phase-field simulation of binary alloy solidification," Journal of Computational Physics, vol. 225, pp. 1271–1287, 2007. doi:10.1016/j.jcp.2007.01.027

[29] R.S. Qin and H.K.D.H Bhadeshia, Phase-field method.Material science and technology.Vol. 26(7), pp. 803-811, 2010.Doi: 10.1179/174328409X453190

[30] R. Kobayashi, J. Warren and W.C. Carter, "Vector-valued phase field model for crystallization and grain boundary formation," Physica D, vol. 119, pp. 415-423, 1998.www.sciencedirect.com/science/article/pii/S0167278998000268

[31] R.S. Qin and H.K.D.H Bhadeshia, "Phase-field study of the crystal morphological evolution of hcp metals," ActaMaterialia, vol. 57, pp. 3382-3390, 2009.doi:10.1016/j.actamat.2009.01.024

[32] I. Loginova, G. Amberg, and J. Agren, "Phase-Field Simulations of non-isothermal binary alloy solidification," Actamateriala, vol. 49, pp. 573–581, 2001. www.sciencedirect.com/science/article/pii/S1359645400003608

[33] H. Assadi, "A phase-field model for non-equilibrium solidification of intermetallics," ActaMaterialia, vol. 55, pp.5225–5235, 2007.doi:10.1016/j.actamat.2007.05.042

[34] W.J. Boettinger, J.A. Warren, C. Beckermann, and A. Karma, 'Phase field simulation of solidification," Ann. Rev. Mater.Res., vol. 32, pp. 163-194, 2002.doi: 10.1146/annurev.matsci.32.101901.155803

[35] T. Pusztai, T. Bortel, G. Gránásy, L., "Phase field modeling of polycrystalline freezing," Materials Science and Engineering A 413–414, pp. 412–417, 2005. doi:10.1016/j.msea.2005.09.057

[36] I. Kovačevič, and B. Sarler, Solution of a phase-field model for dissolution of primary particles in binary aluminum alloys by an r-adaptive mesh-free method. Materials Science and Engineering A 413–414, pp. 423–428, 2005. doi:10.1016/j.msea.2005.09.034

[37] R.F. Almgren, "Second-order phase field asymptotic for unequal conductivities," SIAM J.APPL.MATH, Vol. 59, No. 6, pp. 2086-2107, 1999.http://citeseerx.ist.psu.edu/viewdoc/download?doi=10.1.1.45.9984&rep=rep1&type=pdf

[38] J.A. Warren, W.C. Carter and R. Kobayashi, "A phase Field model of the impingement of solidifying particles," Physica A, vol. 261, pp. 159-166, 1998. www.sciencedirect.com/science/article/pii/S0378437198003811

[39] J. A. Warren, R. Kobayashi, A. E. Lobkovsky and W. C. Carter, "Extending phase field models of solidification to polycrystalline materials," ActaMaterialia, vol. 51, pp. 6035–6058, 2003.Doi: 10.1016/S1359-6454(03)00388-4

[40] T. Takaki, A. Yamanaka and Y. Tomita, "Static recrystallization phase-field simulation based on the predicted subgrain structures," APCOM 2007 in conjunction with EPMESC., Dec. 3-6, 2007. Kyoto, Japan.www.yocky.mes.titech.ac.jp/www2/APCOM2007_takaki.pdf

[41] N.A. Raji,and O.O. Oluwole,"Effectofcolddrawndeformation onmechanical propertiesoflow-carbonsteelduetochangesingrainsizes, "NigerianSociety ofEngineers TechnicalTransactions,Vol.46(3),pp.69-78, 2011.

[42] N.A. Raji,and O.O. Oluwole,"Influence of Degree of Cold-Drawing on the Mechanical Properties of Low Carbon Steel," Materials Sciences and Applications, vol. 2, pp. 1556-1563, 2011. doi:10.4236/msa.2011.211208

[43] J. W. Cahn, P. Fife, and O. Penrose, "A Phase-Field Model for diffusion-induced grain-boundary motion," Actamaterialia, Vol. 45, No. 10, pp. 4397-4413, 1997.http://dx.doi.org/10.1016/S1359-6454(97)00074-8,

[44] N.A. Raji and O.O. Oluwole, "Mechanical Properties of Cold-Drawn Low Carbon Steel for Nail Manufacture: Experimental Observation," Research Journal of Applied Sciences, Engineering and Technology, vol. 5(1, pp. 118-122), 2013. http://maxwellsci.com/print/rjaset/v5-118-122